*31st EPS Conference on Plasma Phys. London, 28 June - 2 July 2004 ECA Vol.**28G**, P-4.174 (2004)*

Critical dynamics of drift-wave turbulence in cylindrical geometry

J.A. Mier, L.García and R.Sánchez

Universidad Carlos III de Madrid, Avda. de la Universidad 30, Leganés, Madrid, Spain

1 Introduction

Drift-wave modes like dissipative trapped electron modes (DTEM) and ion temperature gradient (ITG) modes are suspected to dominate plasma transport in the core region of tokamaks. It has also been suggested that the concept of self-organized criticality (SOC) may be central to the explanation of observed phenomena such as profile stiffness and Bohm scaling. The relevance of SOC has been investigated in resistive interchange turbulence [1, 2], where the critical threshold is set by a pressure gradient, and in ITG turbulence [3] where the threshold is imposed by $\eta_i = L_T/L_n$, the ratio of the density and temperature characteristic length scales. However, in spite of the fact that DTEM turbulence has been extensively studied in a supercritical state [5], its dynamics when the system wanders instead close to its critical point are still unknown. In this work we investigate if SOC should be expected to play any role in this situation by considering a simple model for DTEMs [4], in which the critical threshold is set by a function of L_n and the wave vector $\vec{k}$.

2 Fluid model: Equation and geometry

The DTEM model considered is a paradigm of plasma drift-waves in cylindrical geometry valid for long wavelengths that assumes that the underlying instability mechanism is driven by a population of trapped electrons. The equation for the fluctuating density (normalized to its value at $r = 0$) is [4]:

$$\frac{d}{dt}\left[1-\rho_s^2\nabla_\perp^2\right]\tilde{n} + V_{*n}\frac{1}{r}\frac{\partial\tilde{n}}{\partial\theta} + D_k\frac{1}{r^2}\frac{\partial^2\tilde{n}}{\partial\theta^2} - \frac{c_s^2}{\nu_i}\nabla_\parallel^2\tilde{n} + D\frac{1}{r}\frac{\partial}{\partial r}\left(r\frac{\partial\tilde{n}}{\partial r}\right) - \\ - L_n D_k\left[\nabla_\perp\left(\frac{1}{r}\frac{\partial\tilde{n}}{\partial\theta}\right)\times\hat{z}\right]\cdot\nabla_\perp\tilde{n} = 0 \qquad (1)$$

The cylinder has radius a and length L, and it is considered to be periodic on the z direction. Within it, position is defined relative to the usual unit vectors: $(\hat{r}, \hat{\theta}, \hat{z})$.

3 Equilibrium in steady-state

To study the main features of the critical dynamics of DTEM modes, Eq. 1 is solved after being initialized with small random perturbations to the background equilibrium

profile. These fluctuations act as seed for the instabilities. The system is kept close to its critical point by letting the density profile evolve in time (instead of fixing it to some supercritical value as in [5]). As a result all the modes finally saturate, their growth rates becoming zero as shown in Fig. 1.

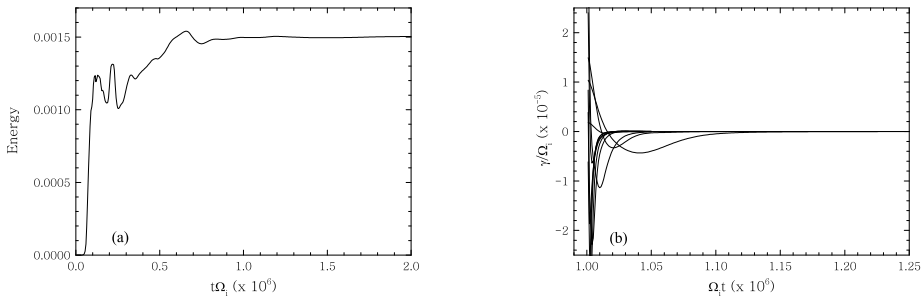

Figure 1: (a) Evolution of energy until saturation; (b) growth-rates after profile relaxation.

4 Transport in steady-state

After the stationary state has been reached, the system is slightly pushed out of equilibrium by imposing an external perturbation. To gain some understanding on how the system reacts, we have first studied the transport properties associated with single pulse gaussian perturbations at different radial positions. Secondly, to investigate the role of SOC dynamics, we investigate the global transport resulting from a continuous random rain of these perturbations.

4.1 Single pulse propagation in steady state

The gaussian perturbations added to the averaged density profile are identified by their amplitude and width. Propagation of both outward (positive pulses initially placed in the inner region) and inward (negative pulses initially placed in the outer region) have been studied (see Fig. 2).

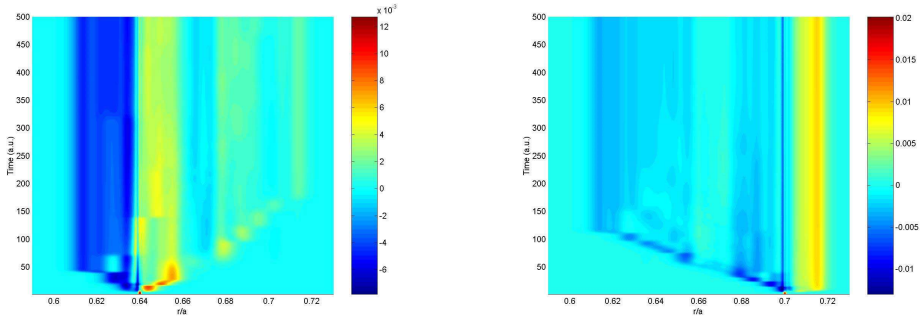

(a) (b)

Figure 2: Incremental density contours (relative to stationary state density) in the t-r plane: (a) Propagation of a positive pulse from $r/a = 0.64$ and (b) a negative pulse from $r/a = 0.7$.

The velocity at which the pulses propagate across the rational surfaces is estimated by means of the maxima of the cross-correlation functions for the temporal traces of the

incremental density relative to the stationary state at different radial positions. It shows that both negative and positive pulses propagate ballistically; $\Delta r \propto V_r \cdot t$, with the radial velocity V_r being strongly dependent on the pulse height (it increases notably when pulse height is doubled), but not so much on its width (it remains approximately constant when the width of the pulse is doubled) as shown in Fig. 3. Moreover, two regions exist in which the pulse velocity takes very different values. These zones are delimited by a discontinuity in the derivative: pulses are stopped when they travel across the position of the lowest-order rational surface $m, n = (3, 2)$. The ballistic character of the propagation supports that transport takes place through the successive destabilization of surfaces, as would be expected in a SOC system.

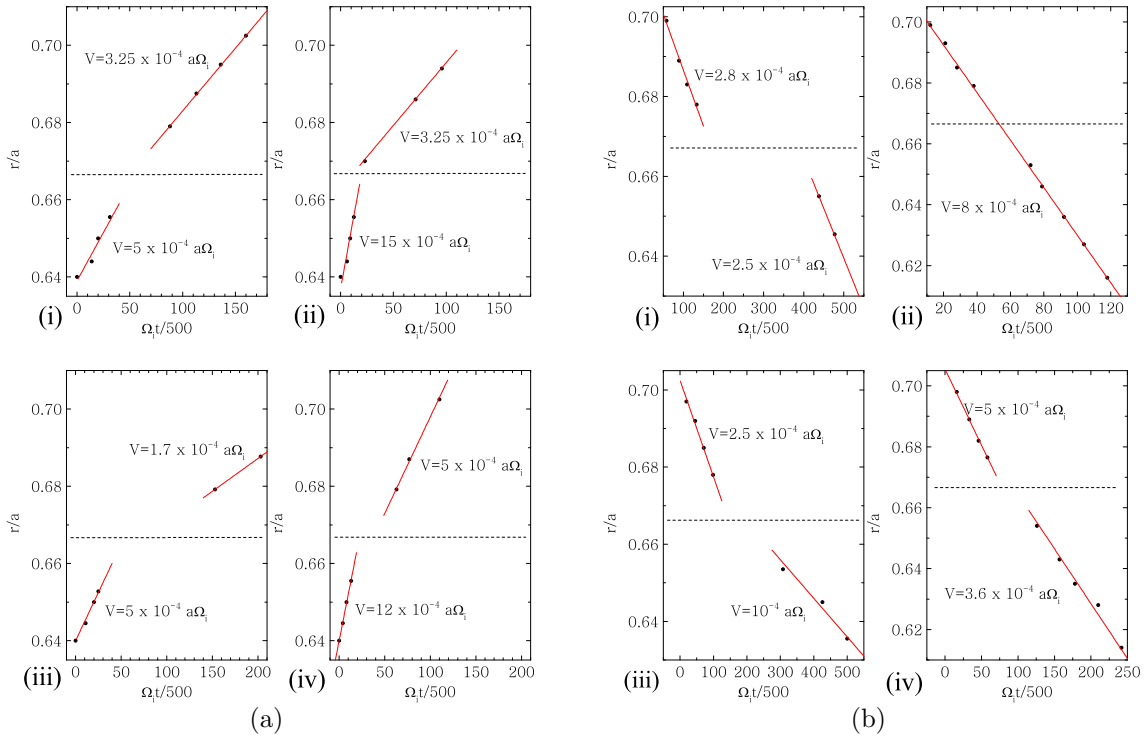

Figure 3: Propagation velocity for (a) positive pulses and (b) negative pulses. Amplitudes (A) relative to the local density and width (W) relative to a are: (i) $A = 0.05$, $W = 0.0005$; (ii) $A = 0.1$, $W = 0.0005$; (iii) $A = 0.05$, $W = 0.001$; (iv) $A = 0.1$, $W = 0.001$.

4.2 Global transport in steady state

The global transport dynamics are now explored by inspecting the evolution of the system steady-state under a continuous noise source. The noise source is built by adding, at each temporal step, a small averaged density perturbation with a probability P_0. The radial position where the perturbation is initially located is randomly chosen in the range where rational surfaces are distributed. These perturbations may trigger local instabilities at the corresponding rational surfaces when the critical value of $1/L_n$ is overcome. As a result, the modes grow nonlinearly transporting density to other nearby locations where new instabilities can then be destabilized. The transport of the excess density is thus

transported outwards and inwards, thus becoming an avalanche-like transport event.
A possible way to explore the character of global transport in the system is by constructing a function of time giving the number of points in the radial grid that are unstable (i.e., where $L_n < L_n^{crit}$). This function estimates the importance of avalanche-like events contribution to the global transport. To look for signatures of SOC dynamics, we calculate the autocorrelation function of this function, which is shown in Fig. 4 for different values of the ambient diffusivity D.

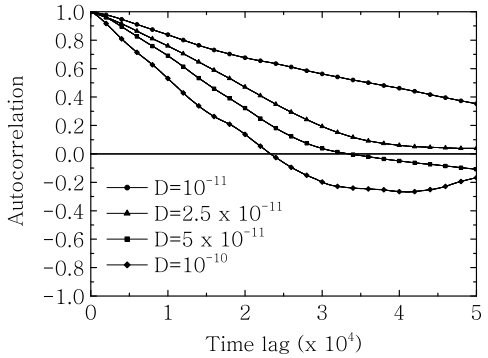

Figure 4: Autocorrelation function of avalanche activity for different values of the diffusivity.

Clearly, the autocorrelation function has a very long tail that is however quickly reduced as the ambient diffusivity increases. At values of diffusivity around $D = 2.5 \cdot 10^{-11}$, diffusive transport already dominates the global dynamics. This behaviour, typical of diffusive-SOC systems [6], is a result of the continuous smoothing of the local density inhomogeneities by diffusion, which pushes the system away from the SOC state.

5 Conclusions

It has been shown that the global transport in a simple model for DTEM turbulence close to its critical point appears to exhibit some signatures characteristic of SOC dynamics. In particular, the propagation of single pulses is associated to the successive destabilization of rational surfaces, being always ballistic for both positive outward-propagating and negative inward-propagating pulses. The radial velocity V_r is strongly dependent on the pulse height. In addition, the interplay between DTEM turbulence and diffusion importantly conditions the efficiency of SOC dynamics to dominate global transport.

References

[1] B. A. Carreras *et al*, *Phys. Plasmas* **3** (8), 2903 (1996).
[2] Y. Sharazin and Ph. Ghendrih, *Phys. Plasmas* **5** (8), 4214 (1998).
[3] X. Garbet and R. E. Waltz, *Phys. Plasmas* **5** (8), 2836 (1998).
[4] B. A. Carreras *et al*, *Phys. Fluids B* **4**, 3115 (1992).
[5] Y. M. Liang *et al*, *Phys. Fluids B* **5**, 1128 (1993).
[6] R. Sánchez, D. E. Newman and B. A. Carreras, *Nucl. Fusion* **41**, 247 (2001).